Structure Formation in Electromagnetically Driven Granular Media

A. Snezhko, I. S. Aranson, and W.-K. Kwok

Materials Science Division, Argonne National Laboratory, 9700 South Cass Avenue, Argonne, Illinois 60439, USA

(Received 20 October 2004; published 18 March 2005)

We report structure formation in submonolayers of magnetic microparticles subjected to periodic electrostatic and magnetic excitations. Depending on the excitation parameters, we observe the formation of a rich variety of structures: clusters, rings, chains, and networks. The dynamics and shapes of the structures are strongly dependent on the amplitude and frequency of the external magnetic field. We find that for pure ac magnetic driving the low-frequency magnetic excitation favors compact clusters, whereas high frequency driving favors chains and netlike structures. An abrupt phase transition from chains to a network phase was observed for a high density of particles.

DOI: 10.1103/PhysRevLett.94.108002 PACS numbers: 45.70.Mg

Large assemblies of macroscopic particles being subjected to external driving, such as vibration, shear, or rotation, exhibit fascinating collective behaviors. Their dynamics are poorly understood, especially when interparticle interactions are strongly dissipative [1]. Additional complications arise when the grain size goes below 0.1 mm, and when nontrivial interactions due to charging or magnetization come into play. When small particles acquire an electric charge or a magnetic moment, the dynamics are governed by the interplay between long-range electromagnetic forces and short-range contact forces. On the other hand, precise electromagnetic excitations can be used to control the morphology of the resulting pattern.

Recently, experimental studies were performed with vibrofluidized magnetic particles [2,3]. Several interesting phase transitions were reported, in particular, the formation of dense two-dimensional clusters and loose quasi-one-dimensional chains and rings. Besides direct interest in the physics of granular media, these studies provide insight into the fundamental problem of dipolar hard sphere fluids where the nature of solid-liquid transitions is still debated [4]. Vibrofluidized magnetic particles can be considered as an extremely simplified model of a ferrofluid, where similar experiments are technically difficult to perform. Previous studies were limited to a very small number of particles (about 1000) due to the intrinsic limitation of the mechanical vibrofluidization technique.

We developed a technique to electrostatically drive fine conducting powders [5,6]. Our approach can effectively deal with extremely fine powders which are not easily controlled by mechanical methods. In addition, our technique allows us to control the ratio between long-range electric forces and short-range collisions by changing the amplitude and frequency of the applied electric field.

In this Letter, we extend our studies towards magnetic microparticles. In addition to electrostatic excitation, we explore the electrostatic driving in the presence of external dc magnetic filed as well as the driving of magnetic particles by an external ac magnetic field. The effect of an additional electric field on the system under magnetic driving is addressed. Our studies reveal a rich diversity of behaviors, including formation of dense immobile clusters and quasi-one-dimensional chains and rings. We provide strong evidence of the first order phase transition from finite length chains of particles to infinite networks as the driving parameters are varied.

The experimental setup is shown in Fig. 1. The design of the cell is similar to that reported earlier [5]. Conductive particles are placed between two horizontal transparent conducting glass plates (12×12 cm with a spacing of 1.5 mm). An external magnetic field is provided by a set of magnetic coils (30 cm in diameter) placed around the cell. To excite the granular media, a voltage of 0–2 kV with a frequency of 0–150 Hz is applied to the plates. This setup is capable of independently creating a dc magnetic field in the range 0–80 Oe and an ac field in the range 0–15 Oe with the frequency 0–300 Hz (for magnetic driving). Spherical nickel particles with an average size of about 90 μm were used. The magnetic moment per particle at the 80 Oe field is 1×10^{-5} emu; the saturated magnetic moment is 2×10^{-4} emu per particle; the saturation field is about 4 kG; the magnetic moment relaxation time is about 7×10^{-4} s. The number of particles was

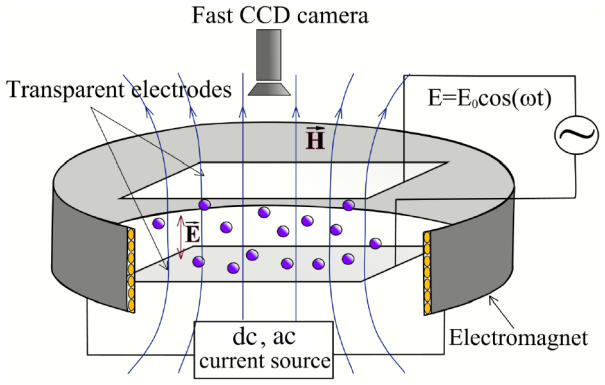

FIG. 1 (color online). Schematic view of the experimental setup.

varied in the range 120 000–300 000. Experiments were also performed with 40 μm sized particles, but no qualitative difference was found. The experiments were performed in air and in nonpolar liquid (toluene).

Electrostatic driving works as follows. Conducting particles acquire an electric charge when they are in contact with the bottom plate of the cell. When the magnitude of the electric field in the cell exceeds some critical value, the upward electric force acting on the charged particle overcomes the gravity and the particles fly towards the upper plate. Upon contact with the upper plate, the particles recharge and fall back to the bottom plate. This process repeats in a cyclical fashion. The elevation of the particles off the bottom plate can be adjusted by the frequency of the applied ac electric field. Pure magnetic driving works in the following way. Magnetic particles with moment $\boldsymbol{M}$ being subjected to an external magnetic field $\boldsymbol{H}$ experience a torque $-[\boldsymbol{M} \times \boldsymbol{H}]$ forcing their magnetic moment to be aligned with the applied magnetic field. It can be done in two ways: (i) the magnetic moment can rotate inside the particle against the internal magnetic anisotropy field, or (ii) the whole particle can rotate to keep the moment aligned with the applied magnetic field. In the latter case, the particle needs to overcome the resistance from the friction and adhesion forces between the particle and the surface of the plate. As the magnitude of the external magnetic field exceeds some critical value, particles begin to rotate by keeping their moment aligned with the field and to move by being driven by the magnetic drag force $\boldsymbol{F}_m = \nabla(\boldsymbol{M}\boldsymbol{H}_{\text{local}})$, where $\boldsymbol{H}_{\text{local}}$ designates the local magnetic field coming from dipolar fields of the neighboring particles and the external magnetic field.

The particles remain immobile on the bottom plate of the cell if the applied electric field is less than some critical value E_1 [5,6]. When the field exceeds a second threshold value, $E_2 > E_1$, the system undergoes a transformation to a gaslike state. Decreasing the electric field E below E_2 ($E > E_1$), small, densely packed clusters begin to nucleate. Clustering is promoted through electrostatic screening (two particles in contact acquire a smaller charge than two separated particles). For magnetic particles the dynamics of cluster formation and critical electric fields E_1, E_2 change due to dipole-dipole magnetic interactions. The phase diagram delineating the primary experimental regimes as a function of applied electric and magnetic fields for 200 000 nickel particles with an average size of 90 μm (about 9% monolayer coverage) in dc magnetic field from 0 to 80 Oe is shown in Fig. 2. The frequency f and the amplitude E of the ac electric field applied to the cell were chosen to provide quasi-two-dimensional motion of the particles ($E < 700$ kV/m, $f = 100$ Hz).

The behavior of the magnetic particles in low external magnetic fields (below 20 Oe) is rather similar to that reported for nonmagnetic conductive particles. The isolated particles are immobile until the electric field exceeds a critical value E_1. At electric field values above E_2, the granular medium transforms into a uniform gaslike phase. Cluster formation is observed in the interval, $E_1 < E < E_2$, in agreement with earlier studies on nonmagnetic granular systems [5,7]. However, the clustering of the magnetic particles is very sensitive to the magnetic field. Clusters formed in the absence of a magnetic field (a) and at a magnetic field of 10 Oe (b) are shown in Fig. 3. The cluster grown in an external magnetic field looks less compact with a very rough edge. Moreover, cluster formation in an external magnetic field is characterized by arrested coarsening due to complete depletion of the gas phase.

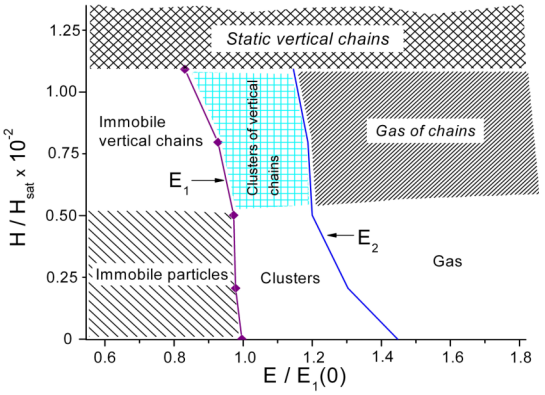

FIG. 2 (color online). Phase diagram for 90 μm nickel particles in the air-filled cell. Magnetic and electric fields are scaled by the saturation field H_{sat} and the first critical field $E_1(H = 0)$, respectively.

We analyzed the growth rates of the clusters at different magnetic fields. The variation of the cluster size for both zero and nonzero external magnetic fields is well described by a simple equation:

$$S(t) = S_\infty\{1 - \exp[-(t - t_0)/\tau]\}. \quad (1)$$

Here S_∞ is the cluster size at $t \to \infty$; t_0 is the time when the cluster nucleates; τ is the growth time. The quantity $[1 - S(t)/S_\infty]$ for the clusters formed at zero field and at 10 Oe is plotted in Fig. 3. Note that for nonmagnetic particles

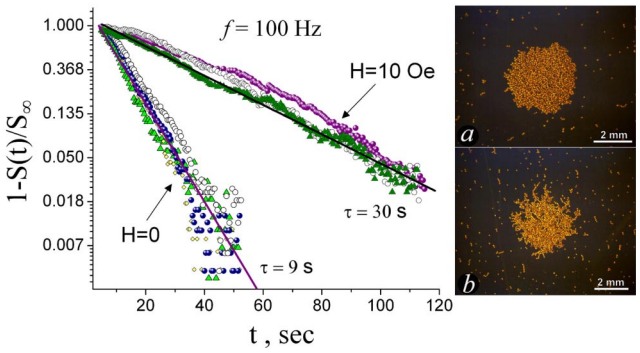

FIG. 3 (color online). Rescaled cluster area vs time at 0 Oe (a) and 10 Oe (b) magnetic fields. Solid lines represent simple functional dependence (1) for different characteristic growth times τ.

exponential relaxation described by Eq. (1) occurs only for the *last surviving cluster*, intermediate clusters show different evolution due to coarsening: small clusters disappear and large grow in their expense [5,6]. The solid lines in Fig. 3 represent the functional dependence of Eq. (1) with corresponding characteristic growth times. The increase of the growth time τ in the presence of an external magnetic field could be explained as follows: Since our particles are multidomain ones, the increase in external magnetic field results in larger particles' magnetic moments (due to the growth of magnetic domains within the particle with orientation along the external field) leading to the amplification of the dipole-dipole interactions. Consequently, the interaction between particles becomes highly anisotropic and increases the characteristic growth time, since (a) aggregation proceeds predominantly through coalescence of chain segments which are less mobile, and since (b) some particles are repelled from the cluster due to unfavorable magnetic moment orientation. The scaling behavior of observed clusters at times far from saturation are in good agreement with those reported for vibrofluidized systems in quasi-two-dimensional regime [7]. For elevated magnetic fields (20–45 Oe), immobile vertical chains consisting of up to four particles were observed when the amplitude of the electric fields was reduced below E_1. The threshold electric field E_1 decreases with increasing external magnetic field since the formation of immobile chains diminishes the effective spacing between cell plates resulting in higher electric field intensity for particles at the top parts of the chains. Upon exceeding E_1, chains start to move and form localized clusters of chains. At amplitudes of electric field above E_2, the system transforms to a gas of short chains. An increase of the magnetic field above 50 Oe creates static long vertical chains touching the upper plate of the cell.

We explored pure ac magnetic driving by placing the magnetic particles into a cell filled with toluene to dampen the kinetic energy in the system. Before each experiment, the system was driven to a gaslike state with an ac electric field in zero magnetic field to create a uniform distribution of particles. Subsequently, the electric field was turned off and the system was subjected to the 15 Oe ac magnetic field. Figure 4 (upper panels) demonstrates some selected structures. The nature of the self-assembled structures is straightforward. Since the local arrangement is dominated by a highly anisotropic dipole-dipole magnetic interaction (a dipole field generated by a particle at a distance comparable to its diameter exceeds 200 Oe), the head-to-tail interaction is the strongest, favoring formation of the quasi-one-dimensional chain structures. It can be shown that a ring is more energetically favorable than a chain if the number of particles in the chain exceeds four [8]. However, to form a ring from a chain, one needs to overcome a strong potential barrier associated with chain bending. Consequently, a more plausible mechanism for

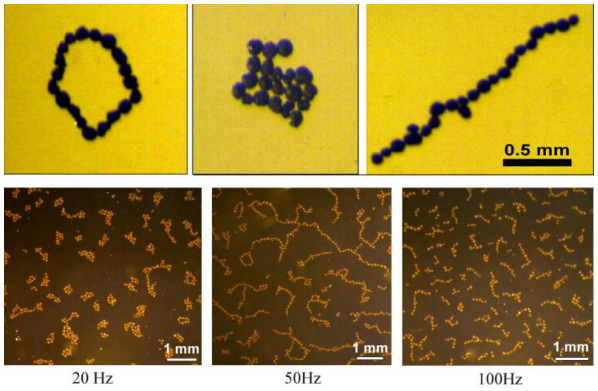

FIG. 4 (color online). Top panels: Structures formed in an external ac magnetic field: rings, compact clusters, and chains of dipoles. Bottom panels: Patterns formed by nickel spheres (5.3% of the surface monolayer coverage) under magnetic driving at 20 Hz (clustered phase), 50 Hz (netlike structure), and 100 Hz (chains phase).

forming a ring is a "fusion" of several short chain segments of appropriate orientation, polarization, and position; see [9]. Chains can also form a compact structure, such as a cluster of dipoles. Such dipole clusters can nucleate in the situation when two neighboring parallel chains have opposite polarization and attract each other to form a cluster.

One can vary the frequency of an ac magnetic field to control the time it takes the particle (or chain segment) to rotate to keep its moment aligned with the local field and move along the local field gradient. There are two characteristic times: one associated with the magnetization of nickel particles and related to domain walls movement ($\sim 7 \times 10^{-4}$ s), and the other related to the mechanical response of the system determined roughly by $\sqrt{I/(MH_0)}$, where I stands for the moment of particle inertia, and H_0 and M designate the amplitude of the external magnetic field and magnetic moment of the particle. The latter gives about 4×10^{-3} s. Thus, if the frequency is too high (above 200 Hz in our case), nothing happens since the mechanical response time is higher than the period of ac magnetic field. By decreasing the frequency, the particles begin to react on an external ac magnetic field and short chains appear in the system. A further decrease of the frequency leads to the creation of more energetically favorable configurations, such as rings and branched chains.

The compact clusters shown in Fig. 4 are initiated by decreasing the frequency of an ac magnetic field. The bottom panels of Fig. 4 show various patterns formed at ac magnetic field of 20, 50, and 100 Hz in the cell with 5.3% surface coverage of Ni particles. Each experiment was started from a randomly dispersed configuration of particles over the bottom plate. Then an ac magnetic field was applied to the cell (no electric field). Clearly, the pattern is determined by the frequency of the ac magnetic field: low-frequency excitations (0–30 Hz) produce a clus-

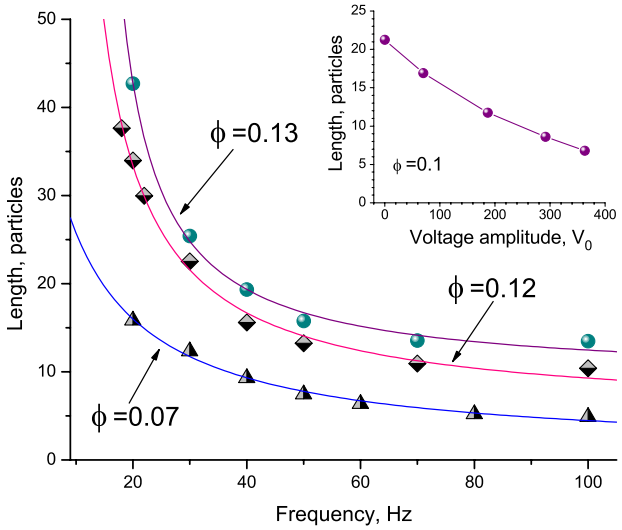

FIG. 5 (color online). Saturated chain length vs frequency of applied 15 Oe ac magnetic field for different amounts of nickel 90 μm particles in the cell. Solid lines are the fits to the expression $y = A + B/(x - f_0)$. Inset: Saturated chain length vs applied ac (100 Hz) electric voltage amplitude for a magnetically driven ($H_{\max} = 15$ Oe; $f = 25$ Hz) system ($\phi \simeq 0.10$).

tered phase; high-frequencies (80–200 Hz) assemble short chains, while intermediate-frequencies favor netlike patterns. The resulting patterns are strongly history dependent. For example, a continuous decrease of the magnetic field frequency from 200 to 10 Hz results in the formation of a netlike structure, in contrast to the formation of clusters obtained by the "relaxation" at the constant frequency of 10 Hz. Denser configurations ($\phi = 0.115$ and 0.133), however, do not exhibit the cluster phase. Instead, a phase transition to the network phase (infinitely long multibranch chains) is observed at low frequencies. To analyze the phase transition, an average chain length as a function of the ac magnetic field frequency is plotted in Fig. 5 for different densities. Data were taken after the system was left to "relax" in the applied field for about 10 min to attain their respective equilibrium state. As the frequency of the magnetic field decreases, the average length of the chains tends to diverge for dense configurations ($\phi = 0.115$ and 0.133) and saturates for less dense ones. The solid lines in the figure are fits to the expression $A + B/(x - f_0)$, where f_0 designates a critical frequency when the system undergoes a phase transition to the netlike phase. The critical frequencies extracted from the fits are 14.10 and 6.11 Hz for $\phi = 0.133$ and $\phi = 0.115$, respectively. The critical frequency for the surface coverage of $\phi = 0.07$ resulted in a negative value, $f_0 = -5.62$ Hz, indicating that there is no transition to the network phase. Indeed, for such low density configurations, compact clusters were observed at low frequencies.

The inset of Fig. 5 demonstrates the effect of an ac electric field on the system of 240 000 Ni particles ($\phi \simeq 0.10$) in the ac magnetic field ($H_{\max} = 15$ Oe; $f = 25$ Hz). The frequency of the electric field was kept at 100 Hz to provide mostly two-dimensional motion. The average length of the chain decreases with increasing ac electric field, suggesting that the latter acts as temperature.

We studied the self-assembly of magnetic microparticles in ac electric and magnetic fields. Excitation of the system by an ac magnetic field revealed a variety of patterns that can be controlled by adjusting the frequency and the amplitude of the field. We found that at low particle densities the low-frequency magnetic excitation favors cluster phase formation, while high frequency excitation favors chains and netlike structures. For denser configurations, an abrupt transition to the network phase was observed.

We thank Ulrich Welp and John Mitchell for help with magnetization measurements. This research was supported by the U.S. DOE, Grant No. W-31-109-ENG-38.

[1] L. Kadanoff, Rev. Mod. Phys. **71**, 435 (1999); H. Jaeger *et al.*, Rev. Mod. Phys. **68**, 1259 (1996).
[2] D. L. Blair and A. Kudrolli, Phys. Rev. E **67**, 021302 (2003).
[3] J. Stambaugh *et al.*, Phys. Rev. E **68**, 026207 (2003); **70**, 031304 (2004).
[4] P. G. de Gennes and P. A. Pincus, Phys. Kondens. Mater. **11**, 189 (1970); Y. Levin, Phys. Rev. Lett. **83**, 1159 (1999); J. M. Tavares *et al.*, Phys. Rev. E **65**, 061201 (2002); Ph. J. Camp *et al.*, Phys. Rev. Lett. **84**, 115 (2000); A. Yu. Zubarev *et al.*, Phys. Rev. E **65**, 061406 (2002).
[5] I. S. Aranson *et al.*, Phys. Rev. Lett. **84**, 3306 (2000); **88**, 204301 (2002).
[6] M. V. Sapozhnikov *et al.*, Phys. Rev. Lett. **90**, 114301 (2003).
[7] M. V. Sapozhnikov *et al.*, Phys. Rev. E **67**, 010302(R) (2003).
[8] Weijia Wen *et al.*, Phys. Rev. E **59**, R4758 (1999); F. Kun *et al.*, Phys. Rev. E **64**, 061503 (2001).
[9] See EPAPS Document No. E-PRLTAO-94-024514 for movies illustrating the formation of structures. A direct link to this document may be found in the online article's HTML reference section. The document may also be reached via the EPAPS homepage (http://www.aip.org/pubserves/epaps.html) or from ftp.aip.org in the directory /epaps/. See the EPAPS homepage for more information.